SCIENCE CHINA
Technological Sciences

•Article•

June 2021 Vol.64 No.6: 1276–1284
https://doi.org/10.1007/s11431-020-1740-5

First-principles study of multiple-site substitutions of alloying elements in Ni-based single crystal superalloys

SUN JunXi[1,2], DU Wan[2], XIAO Bin[2], WU YuQin[2], LIU Yi[1,2*] & ZHANG TongYi[1,2*]

[1] *State Key Laboratory of Advanced Special Steel, Shanghai University, Shanghai 200444, China;*
[2] *Materials Genome Institute, Shanghai University, Shanghai 200444, China*

Received June 16, 2020; accepted October 20, 2020; published online April 30, 2021

The development of Ni-based single crystal superalloys relies heavily on the composition design with the addition of critical alloying elements, e.g., Re and Ru. Understanding the role of alloying effects require to know the configurations of the alloying element distribution between γ-Ni and γ′-Ni_3Al phases and among various non-equivalent sites. This work employed first-principles density functional theory calculations to study the preference of phase and site occupancy of 11 alloying elements including Al and transition metal elements: 3d (Ti, Cr, Co, Ni), 4d (Mo, Ru), and 5d (Hf, Ta, W, Re) in Ni and Ni_3Al. We calculated the substitution energies of 1298 triple-site doping configurations including 286 NiNiNi site doping of Ni, 726 AlNiNi site doping, and 286 NiNiNi site doping of Ni_3Al with alloying elements Ni, Co, Ru, Cr, Re, Mo, W, Al, Ti, Ta, and Hf. In the dual-site and triple-site doping of Ni and Ni_3Al, all studied alloying elements preferred to occupy Ni phase rather than Ni_3Al phase. We found that the most stable defect complexes often contained the favorable substitutions of Al, Ti, Ta, and Hf for the Ni sites that stabilized the alloying elements doping at the other one or two nearest neighbor sites. The co-substitutions of various alloying elements at multiple sites are critical to understanding the strengthening mechanism of alloying elements in Ni-based single crystal superalloys.

Ni-based single crystal superalloy, first-principles density functional theory calculations, phase and site occupancy, substitution energy, alloy design

Citation: Sun J X, Du W, Xiao B, et al. First-principles study of multiple-site substitutions of alloying elements in Ni-based single crystal superalloys. Sci China Tech Sci, 2021, 64: 1276–1284, https://doi.org/10.1007/s11431-020-1740-5

1 Introduction

Ni-based superalloys have excellent high-temperature mechanical properties, good corrosion resistance, and oxidation resistance, mainly used in four major components of combustion chambers, guide vanes, turbine blades, and turbine disks of advanced aviation engines and gas turbine [1,2]. The chemical composition of Ni-based superalloys is a complex combination of more than 10 alloying elements and the design of alloy composition plays a key role in the development of superalloys for each generation. Due to the additions of Re and Ru elements, the recent generations of superalloys have been continuously developed [3,4]. A modern commercial superalloy normally contains more than 10 transition metal alloying elements that have important effects on the mechanical strength and creep properties of the Ni-based superalloy [5]. To understand the strengthening mechanism of the alloying elements, it is necessary to understand the occupancy and distribution of alloying elements in γ-Ni and γ′-Ni_3Al phases. The large number of doping elements in the superalloy lead to the numerous possible arrangement and combination of the alloying elements considering the element types, occupancy sites, distance, concentration, and interface (γ/γ′), etc. [6–10]. The systematic studies of the alloying effects on the occupancy become fundamentally important but very challenging.

*Corresponding authors (email: yiliu@shu.edu.cn; zhangty@shu.edu.cn)

The first-principle density functional theory (DFT) calculations have been used to study the occupancy preference of alloying elements, critical to understanding the roles of doping elements in γ-Ni and γ′-Ni_3Al [11–16]. Except for a few elements with a tendency of occupying Ni sites, most alloying elements prefer to occupy Al site in Ni_3Al [17–20]. So far most of the first-principles studies focused on the doping at a single-site with much fewer studies on a dual-site doping in Ni and Ni_3Al. However, the multi-component engineering alloys require the understanding of doping at multiple-sites including the correlation effects among the multiple alloying elements. Mottura et al. [21] did atom probe tomography analysis and detected the enrichment of Re in the γ matrix phase close to the matrix/precipitate (γ/γ′) phase boundaries. Liu et al. [22] found that the 3d solute elements, except for Ti, partition to γ phase, whereas 4d and 5d solute elements, except for Ru, Rh, and Ir, prefer to occupy γ′ phase in the ternary model of superalloys. Tan et al. [23] found that a bimodal size distribution of γ′ precipitates with large primary γ′ precipitates and numerous smaller secondary γ′ precipitates were obtained after the isothermal aging at 1100°C.

This work employed the first-principles DFT calculations to study systematically the effects of multiple alloying elements doping at up to triple substitution sites in Ni and Ni_3Al, respectively. Specifically, a total of 1298 substitution configurations were constructed considering single-site doping, dual-site doping, and triple-site doping in Ni and Ni_3Al, respectively, including 726 AlNiNi site doping systems ($X_{Al}Y_{Ni}Z_{Ni}$@Ni_3Al) in γ′-Ni_3Al, 286 NiNiNi site doping systems ($X_{Ni}Y_{Ni}Z_{Ni}$@Ni_3Al) in γ′-Ni_3Al, and 286 NiNiNi site doping systems ($X_{Ni}Y_{Ni}Z_{Ni}$@Ni) in γ-Ni. The substitution energies calculated by first-principles calculations were used to determine the preference of phase and site occupancy in single-site doping, dual-site doping, and triple-site doping in γ′-Ni_3Al and γ-Ni. We discussed the stable defect complex configurations that are possibly relevant to the strengthening mechanism of alloying elements in Ni-based single crystal alloy.

2 Computational method and models

2.1 Computational method

In this work, we carried out the first-principles DFT calculations using Vienna *ab initio* simulation package (VASP) [24] where the interactions between core and electrons were described by the pseudopotential of projection-augmented wave (PAW) [25,26]. The exchange correlation functional adopted the generalized gradient approximation of Perdew, Burke and Ernzerhof (GGA-PBE) [19]. The electronic wave functions were expanded using plane waves with a kinetic-energy cutoff of 350 eV. Monkhorst-Pack *k*-point mesh (5×5×5) was used for the Brillouin zone integrations [27]. The spin-polarized calculations were used to include the effect of magnetism. The energy convergence criterion was 10^{-5} eV in the self-consistent field calculation of electrons. All atoms within the supercell were fully relaxed in the structure optimization until the local force on each atom was less than 0.01 eV/Å while fixing the lattice parameters of the relaxed pristine Ni and Ni_3Al structures.

2.2 Substitution model

In this work, both γ-Ni and γ′-Ni_3Al phases were modelled using 2×2×2 Ni and Ni_3Al supercells with 32 atoms, respectively, which ignored the interaction between γ-Ni and γ′-Ni_3Al phases at γ/γ′ interface. To study the alloying effects we built triple-site substitution models (XYZ) by substituting up to three the nearest neighbor sites with 11 alloying elements: X, Y, or Z= Al and Co, Cr, Hf, Mo, Ni, Re, Ru, Ta, Ti, W (3d, 4d, and 5d transition metals). In the pristine supercells there is one non-equivalent Ni site in γ-Ni while there are two non-equivalent Ni and Al sites in γ′-Ni_3Al, respectively (Figure 1).

All combinations of the three non-equivalent substitution sites were considered in the three triple-site (TS) models of γ-Ni and γ′-Ni_3Al phases. The first TS model included one Al and two Ni sites that are the nearest neighbors to each other in Ni_3Al model, dubbed $X_{Al}Y_{Ni}Z_{Ni}$@Ni_3Al model where the Ni and Al at lower cases indicate the original lattice sites while X, Y, and Z represent the studied alloying elements for substitution in Ni_3Al phase. The second TS model substituted the three nearest neighbor Ni sites in Ni_3Al phase, dubbed $X_{Ni}Y_{Ni}Z_{Ni}$@Ni_3Al. The third TS model contained the three nearest neighbor Ni sites for substitution in γ-Ni phase, dubbed $X_{Ni}Y_{Ni}Z_{Ni}$@Ni. In these substitution models, the elements X, Y, and Z were chosen from 11 alloying elements Al and Co, Cr, Hf, Mo, Ni, Re, Ru, Ta, Ti, W (3d, 4d, and 5d transition metals). In total 1298 substitution configurations were constructed to describe single-site (SS) doping, dual-site (DS) doping, and triple-site (TS) doping in γ′-Ni_3Al and γ-Ni models, respectively, including 286 NiNiNi site doping configurations ($X_{Ni}Y_{Ni}Z_{Ni}$@Ni) of Ni, 726 AlNiNi site doping configurations ($X_{Al}Y_{Ni}Z_{Ni}$@Ni_3Al), and 286 NiNiNi site doping configurations ($X_{Ni}Y_{Ni}Z_{Ni}$@Ni_3Al) of Ni_3Al.

2.3 Substitution energy of doping elements

To evaluate the changes of total energies due to the substitutions for up to the three doping sites, we calculated the single-site substitution energy (E_{SS}), dual-site substitution energy (E_{DS}), and triple-site substitution energy (E_{TS}). There are two non-equivalent configurations in the single-site substitution, two non-equivalent configurations in the dual-site substitution, and one non-equivalent configuration in the

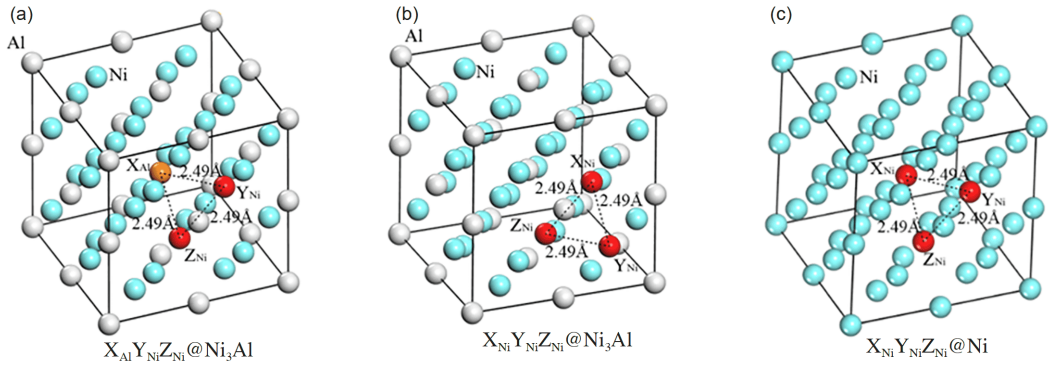

Figure 1 (Color online) Atomic structure models of 2×2×2 supercells of (a) $X_{Al}Y_{Ni}Z_{Ni}$@Ni_3Al, (b) $X_{Ni}Y_{Ni}Z_{Ni}$@Ni_3Al and (c) $X_{Ni}Y_{Ni}Z_{Ni}$@Ni.

triple-site substitution.

When the Ni site is substituted, the single-site substitution energy E_{SS} is defined as follows:

$$E_{SS} = E_{tot} + E_{Ni} - E_{pure} - E_{m1}. \quad (1)$$

When the Al site is substituted, E_{SS} is defined as follows:

$$E_{SS} = E_{tot} + E_{Al} - E_{pure} - E_{m1}. \quad (2)$$

When the two Ni sites are substituted, the dual-site substitution energy, E_{DS} is defined as

$$E_{DS} = E_{tot} + 2E_{Ni} - E_{pure} - E_{m1} - E_{m2}. \quad (3)$$

When one Ni site and one Al site are substituted, E_{DS} is defined as follows:

$$E_{DS} = E_{tot} + E_{Ni} + E_{Al} - E_{pure} - E_{m1} - E_{m2}. \quad (4)$$

The triple-site substitution energy E_{TS} is defined as

$$E_{TS} = E_{tot} + 2E_{Ni} + E_{Al} - E_{pure} - E_{m1} - E_{m2} - E_{m3}. \quad (5)$$

In the equations above, E_{tot} is the total energy of Ni_3Al system after triple-site substitution calculated by DFT; E_{pure} is the energy of pristine γ′-Ni_3Al or γ-Ni without substitution; E_m(m= Al, Co, Cr, Hf, Mo, Ni, Re, Ru, Ta, Ti, W) is the total energy per atom of the pure crystal of each alloying element, e.g., E_{Ni} is the total energy per atom of pure Ni crystal. The total energies of 11 pure crystals are listed in Table S1 of Supporting Information (SI).

2.4 Normalized transfer energy of doping elements

To describe quantitatively the tendency of single-site doping in Ni_3Al, Ruban et al. [28] proposed a normalized transfer energy ($E^X_{B\to A}$) to judge the preference of the site occupancy of doping element X. First, consider a binary ordered alloy A_kB_m, e.g., Ni_3Al in this study where A and B represent Ni and Al, respectively, and k=3, m=1. Then, the energies of two basic processes are considered: the energy moving an X atom from site B to site A is defined as $E^X_{B\to A}$ and the energy moving an X atom from site A to site B is defined as $E^X_{A\to B}$, defined as follows:

$$E^X_{B\to A} = E^X(A) - E^X(B) + E_{ant}(B), \quad (6)$$

$$E^X_{A\to B} = E^X(B) - E^X(A) + E_{ant}(A), \quad (7)$$

where $E^X(A)$ and $E^X(B)$ are the substitution energies of the doping element X added to the sub-lattice A and B, respectively. $E^X(A)$ means that X occupies site A (Ni), corresponding to $Al_{Al}X_{Ni}Ni_{Ni}$@Ni_3Al configuration in this work; $E^X(B)$ means that X occupies site B (Al), corresponding to $X_{Al}Ni_{Ni}Ni_{Ni}$@Ni_3Al configuration. $E_{ant}(A)$ and $E_{ant}(B)$ are the formation energies of the antisite defect energies of the sub-lattice A and B, respectively. $E_{ant}(A)$ means that B (Al) occupies site A (Ni), corresponding to $Al_{Al}Al_{Ni}Ni_{Ni}$@Ni_3Al. $E_{ant}(B)$ means that A (Ni) occupies site B (Al), corresponding to $Ni_{Al}Ni_{Ni}Ni_{Ni}$@Ni_3Al.

Adding eqs. (6) and (7), we obtain

$$E^X_{B\to A} + E^X_{A\to B} = E_{ant}(B) + E_{ant}(A) = E^{xc}_{ant}, \quad (8)$$

where E^{xc}_{ant} is the exchange energy of an antisite defect. Then we obtain the normalized $\tilde{E}^X_{B\to A}$:

$$\tilde{E}^X_{B\to A} = E^X_{B\to A} / E^{xc}_{ant}. \quad (9)$$

$\tilde{E}^X_{B\to A}$ can be used to describe the tendency of doping elements. The criteria of preference of site occupancy can be classified into four categories as follows:

I: $\tilde{E}^X_{B\to A} < 0$ indicates strong site A preference;
II: $\tilde{E}^X_{B\to A} > 1$ indicates strong site B preference;
III: $0 < \tilde{E}^X_{B\to A} < 0.5$ indicates weak site A preference;
IV: $0.5 < \tilde{E}^X_{B\to A} < 1$ indicates weak site B preference. (10)

We calculated the formation energies of the antisite defects in Ni_3Al and obtained $E_{ant}A = -0.885$ eV for Al_{Ni} antisite, $E_{ant}B = 2.036$ eV for Ni_{Al} anitsite, respectively. This indicates that it is energetically favorable to form Al_{Ni} antisite defect but the formation of Ni_{Al} is unfavorable in Ni_3Al

phase. The exchange energy of the antisite defects in Ni_3Al is the summation of the two antisite defects based on eq. (8). E_{ant}^{xc}= 1.15 eV (GGA-PBE) calculated in this study is very close to the calculated literature results: 1.12 eV by Jiang [9] (GGA-PW91) and 1.10 eV by Zhao et al. [10] (GGA-PBE). These DFT values were smaller than that of 2.00 eV calculated by Ruban et al. [28] using TB-LMTO-ASA-CPA method based on phenomenological order energy expansion. All these calculated exchange energy results indicate that it is energetically unfavorable for the exchange of Al and Ni to form a pair of antisite defects, Al_{Ni} and Ni_{Al}, in Ni_3Al.

3 Results and discussion

3.1 Substitution energies of 11 alloying elements

3.1.1 Re element

(1) Single-site doping with Re

The single-site doping configurations considered the three non-equivalent substitution sites in γ-Ni and γ′-Ni_3Al, namely, Al and Ni sites in γ′-Ni_3Al and Ni site in γ-Ni. When Re was a single-site doping element and the other elements remained unchanged, we calculated the single-site substitution energies E_{SS} of Re doping: $E_{SS}(Re_{Al}Ni_{Ni}Ni_{Ni}@Ni_3Al)$= 0.030 eV, $E_{SS}(Al_{Al}Re_{Ni}Ni_{Ni}@Ni_3Al)$=1.515 eV, $E_{SS}(Re_{Ni}Ni_{Ni}Ni_{Ni}@Ni)$= 0.194 eV. Based on the enthalpy criterion the configuration with less positive or more negative substitution energy, described as larger substitution energy hereafter, means a more stable structure with larger preference of occupancy of doping elements at ground state. Thus Re element tends to occupy the Al site of Ni_3Al with a slightly positive substitution energy in the single-site doping, more stable than the other two doping sites.

(2) Dual-site doping with Re

The dual-site doping configurations considered up to two doping elements, enabling the examination of the correlation effects between the co-doping alloying elements. When Re and Y were used as the two substitution elements in the dual-site doping, there are four non-equivalent dual-site substitution configurations: $X_{Al}Y_{Ni}Ni_{Ni}@Ni_3Al$, $Al_{Al}X_{Ni}Y_{Ni}@Ni_3Al$, $X_{Ni}Y_{Ni}Ni_{Ni}@Ni_3Al$, and $X_{Ni}Y_{Ni}Ni_{Ni}@Ni$.

Figure 2 shows the dual-site substitution energies of 21 ReY or XRe substitution for the four non-equivalent site pairs of Ni and Ni_3Al where X and Y are one of the 11 alloying elements studied in this work. The E_{DS} of $Re_{Ni}Y_{Ni}Ni_{Ni}@Ni$ configurations were larger than those of the other three configurations independent of the type of X or Y elements, except for the $Re_{Al}Ni_{Ni}Ni_{Ni}@Ni_3Al$ configuration that is the same as the most stable single-site Re doping case discussed above.

The introduction of one more doping element changed the preference of Re occupancy from Ni_3Al phase to γ-Ni phase,

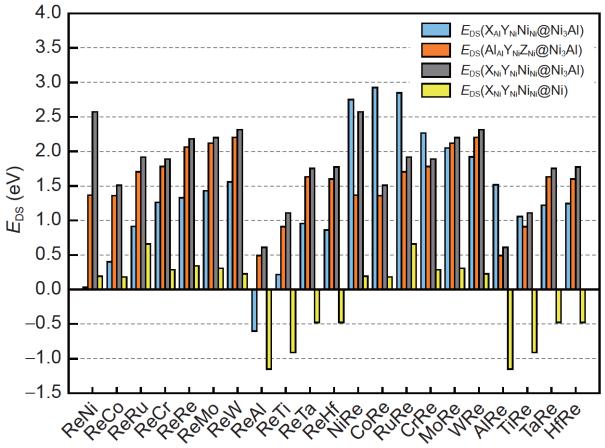

Figure 2 (Color online) Dual-site substitution energies of 21 ReY or XRe substitutions for the four non-equivalent dual-site configurations of Ni and Ni_3Al where X and Y are one of the 11 alloying elements. X, Y = Ni, Co, Ru, Cr, Re, Mo, W, Al, Ti, Ta, and Hf.

indicating that the correlation of the two doping elements is crucial. Specifically, the E_{DS} became negative in Ni phase when X, Y= Al, Ti, Ta, and Hf. The ReAl substitution in Ni is the most stable dual-site doping configuration with E_{DS} ($Re_{Ni}Al_{Ni}Ni_{Ni}@Ni$) = −1.154 eV. Compared with the single-site substitution energies $E_{SS}(Re_{Ni}Ni_{Ni}Ni_{Ni}@Ni)$ = 0.194 eV and $E_{SS}(Al_{Ni}Ni_{Ni}Ni_{Ni}@Ni)$ = −1.511 eV, we understood that the major stabilization effect came from the Al_{Ni} substitution. Similarly, Ti, Ta, and Hf can also serve as the second doping elements to stabilize Re substitution in Ni. Also, the ReAl pair substitution in $Re_{Al}Al_{Ni}Ni_{Ni}@Ni_3Al$ configuration had negative E_{DS} indicating that the antisite defect Al_{Ni} in Ni_3Al prompted Re substitution for Al. The formation of the antisite defect Al_{Ni} is energetically preferable with the formation energy −0.885 eV in Ni_3Al. If Re is doped into Ni_3Al, Re preferred to occupy Al sites rather than Ni sites. These results show that the ReAl pair substitutions are relatively stable doping configurations in both Ni and Ni_3Al.

(3) Triple-site doping with Re

The triple-site doping configurations considered up to three different alloying elements that are the nearest neighbors each other in Ni and Ni_3Al, allowing the examination of the correlation effects among three doping elements. When Re, Y, and Z were adopted as the three doping elements in triple-site doping, there are four non-equivalent triple-site substitution configurations: $Re_{Al}Y_{Ni}Z_{Ni}@Ni_3Al$, $X_{Al}Re_{Ni}Z_{Ni}@Ni_3Al$, $Re_{Ni}Y_{Ni}Z_{Ni}@Ni_3Al$, and $Re_{Ni}Y_{Ni}Z_{Ni}@Ni$.

Figure 3 show the triple-site substitution energies of ReYZ or XReZ substitutions for the four non-equivalent triple-site configurations of Ni and Ni_3Al: $Re_{Al}Y_{Ni}Z_{Ni}@Ni_3Al$, $X_{Al}Re_{Ni}Z_{Ni}@Ni_3Al$, $Re_{Ni}Y_{Ni}Z_{Ni}@Ni_3Al$, and $Re_{Ni}Y_{Ni}Z_{Ni}@Ni$ where X, Y, or Z are one of the 11 alloying elements studied in this work, sorted in the increasing order of metal radii. Among the four triple-site substitution configurations con-

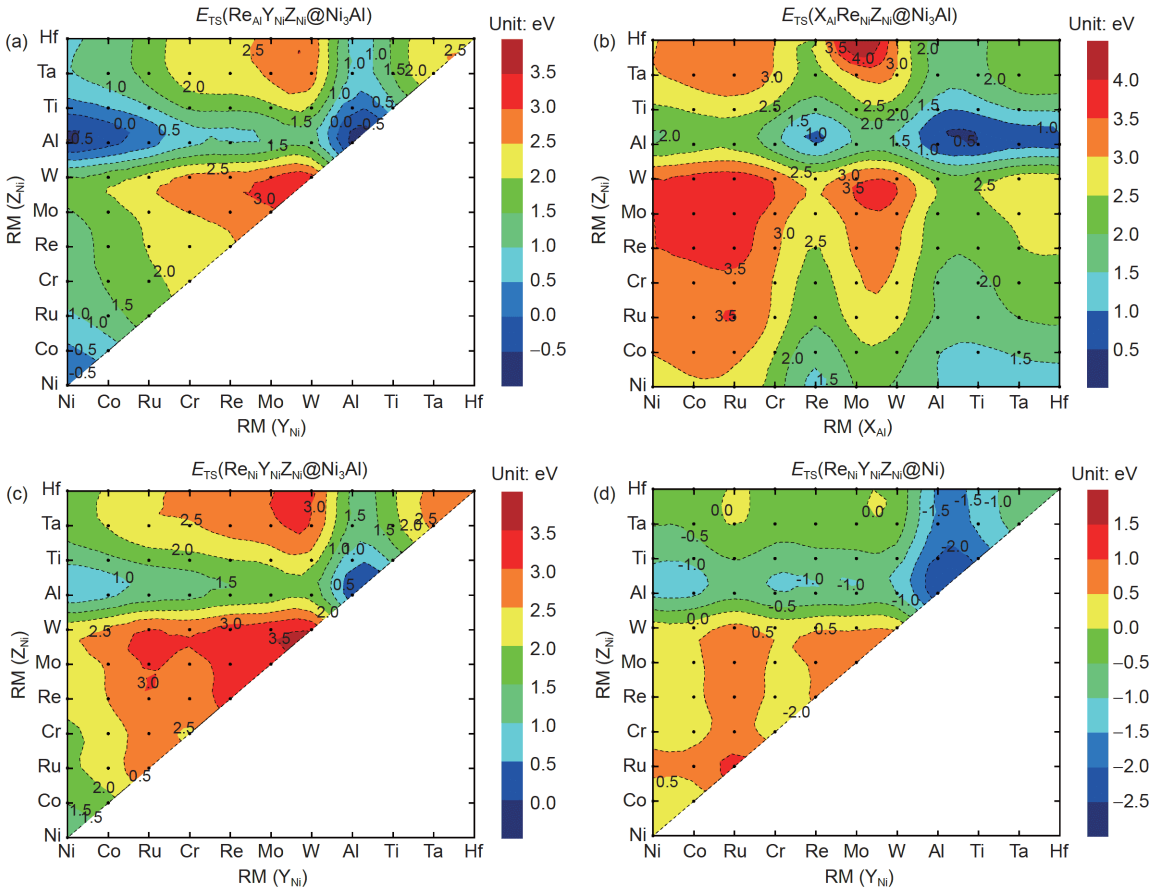

Figure 3 (Color online) Triple-site substitution energies of ReYZ or XReZ substitution for the four non-equivalent triple-site configurations of Ni and NizAl. (a) $Re_{Al}Y_{Ni}Z_{Ni}@Ni_3Al$, (b) $X_{Al}Re_{Ni}Z_{Ni}@Ni_3Al$, (c) $Re_{Ni}Y_{Ni}Z_{Ni}@Ni_3zAl$, and (d) $Re_{Ni}Y_{Ni}Z_{Ni}@Ni$ where X, Y, and Z are one of the 11 alloying elements. X, Y, Z = Ni, Co, Ru, Cr, Re, Mo, W, Al, Ti, Ta, and Hf, sorted in the increasing order of metal radii.

taining Re, $Re_{Ni}Y_{Ni}Z_{Ni}@Ni$ are generally more stable than the other three configurations, indicating that Re prefers to occupy Ni phase rather than Ni_3Al phase in the triple-site doping. $Re_{Ni}Y_{Ni}Z_{Ni}@Ni$ had negative E_{TS} when Y or/and Z= Al, Ti, Ta, and Hf with large metal radii. Among the four triple-site substitution configurations, $Re_{Ni}Al_{Ni}Al_{Ni}@Ni$ had the largest E_{TS}= −2.340 eV, followed by $Re_{Al}Al_{Ni}Al_{Ni}@Ni_3Al$ (−0.686 eV), $Re_{Ni}Al_{Ni}Al_{Ni}@Ni_3Al$ (0.170 eV), and $Ti_{Al}Re_{Ni}Al_{Ni}@Ni_3Al$ (0.497 eV). We found again that the antisite defect Al_{Ni} stabilized Re substitution in both Ni and Ni_3Al in the triple-site doping configurations, consistent with the results of the dual-site doping. Re prefered to occupy Al sites rather than Ni sites in the triple-site doping of Ni_3Al, consistent with the results of dual-site doping.

3.1.2 Ru element

(1) Single-site doping with Ru

When Ru was a single-site doping element, we calculated the single-site substitution energies E_{SS} of Ru doping: E_{SS} ($Ru_{Al}Ni_{Ni}Ni_{Ni}@Ni_3Al$)= 2.103 eV, E_{SS} ($Al_{Al}Ru_{Ni}Ni_{Ni}@Ni_3Al$) = 0.991 eV, E_{SS} ($Ru_{Ni}Ni_{Ni}Ni_{Ni}@Ni$)= 0.539 eV. Thus Ru element preferred to occupy Ni phase rather than Ni_3Al phase in the single-site doping, opposite to the phase preference of Re occupancy. If Ru was doped into Ni_3Al, Ru preferred to occupy Ni site rather than Al site. The E_{SS} of Ru were all positive, generally smaller than those of Re, indicating the less stabilization effects to both Ni and Ni_3Al as a single-doping element compared with Re.

(2) Dual-site doping with Ru

When Ru and X or Y were the two substitution elements in the dual-site doping, there are four non-equivalent dual-site substitution configurations: $X_{Al}Y_{Ni}Ni_{Ni}@Ni_3Al$, $Al_{Al}X_{Ni}Y_{Ni}@Ni_3Al$, $X_{Ni}Y_{Ni}Ni_{Ni}@Ni_3Al$, and $X_{Ni}Y_{Ni}Ni_{Ni}@Ni$.

Figure 4 shows the dual-site substitution energies of 21 RuY or XRu substitution for the four non-equivalent site pairs of Ni and Ni_3Al where X or Y are one of the 11 alloying elements studied in this work. The E_{DS} of $Ru_{Ni}Y_{Ni}Ni_{Ni}@Ni$ configurations were larger than those of the other three configurations independent of the type of X or Y elements, indicating that Ru preferred to occupy Ni phase rather than Ni_3Al phase, consistent with the results of single-site doping. Specifically, the E_{DS} were negative in Ni when X, Y= Al, Ti, Ta, and Hf. Similar to ReAl, the RuAl substitution in Ni was most stable dual-site doping configuration with E_{DS}(Ru_{Ni}-

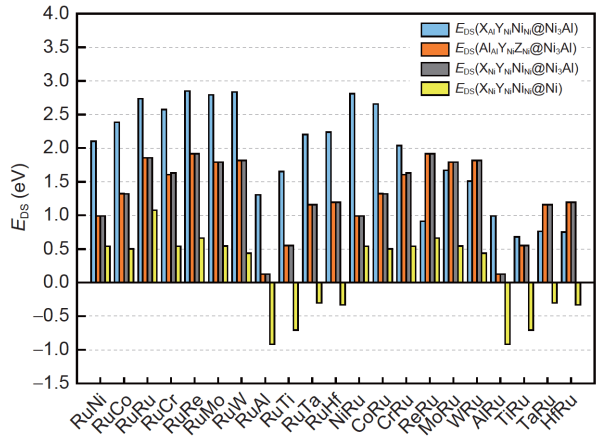

Figure 4 (Color online) Dual-site substitution energies of 21 RuY or XRu substitutions for the four non-equivalent dual-site configurations of Ni and Ni_3Al where X and Y are one of the 11 alloying elements. X, Y= Ni, Co, Ru, Cr, Re, Mo, W, Al, Ti, Ta, and Hf.

$Al_{Ni}Ni_{Ni}$@Ni) = −0.919 eV. Compared with the single-site substitution energies $E_{SS}(Ru_{Ni}Ni_{Ni}Ni_{Ni}@Ni)$ = 0.539 eV and $E_{SS}(Al_{Ni}Ni_{Ni}Ni_{Ni}@Ni)$ = −1.511 eV, we found that the major stabilization effect also came from the Al_{Ni} substitution. Similarly, Ti, Ta, and Hf stabilized Ru substitution in Ni as the second doping elements. These results show that the RuAl pair substitutions are relatively stable doping configurations in Ni. If Ru was doped into Ni_3Al, Ru preferred to occupy Ni sites rather than Al sites, opposite to the preference of Re occupancy in Ni_3Al. The antisite defect Al_{Ni} in Ni_3Al prompted Ru substitution for Ni. These results show that the RuAl pair substitutions are relatively stable doping configuration in both Ni and Ni_3Al.

(3) Triple-site doping with Ru

When Ru, Y, and Z were adopted as the three doping elements in triple-site doping, there are four non-equivalent triple-site substitution configurations: $Ru_{Al}Y_{Ni}Z_{Ni}@Ni_3Al$, $X_{Al}Ru_{Ni}Z_{Ni}@Ni_3Al$, $Ru_{Ni}Y_{Ni}Z_{Ni}@Ni_3Al$, and $Ru_{Ni}Y_{Ni}Z_{Ni}@$ Ni. Figure 5 show the triple-site substitution energies of RuYZ or XRuZ substitution for the four non-equivalent triple-site doping configurations of Ni and Ni_3Al: $Ru_{Al}Y_{Ni}Z_{Ni}$ @Ni_3Al, $X_{Al}Ru_{Ni}Z_{Ni}@Ni_3Al$, $Ru_{Ni}Y_{Ni}Z_{Ni}@Ni_3Al$, and $Ru_{Ni}Y_{Ni}Z_{Ni}@$Ni where X, Y, or Z are one of the 11 alloying elements studied in this work, sorted in the increasing order of metal radii. Among the four triple-site substitution con-

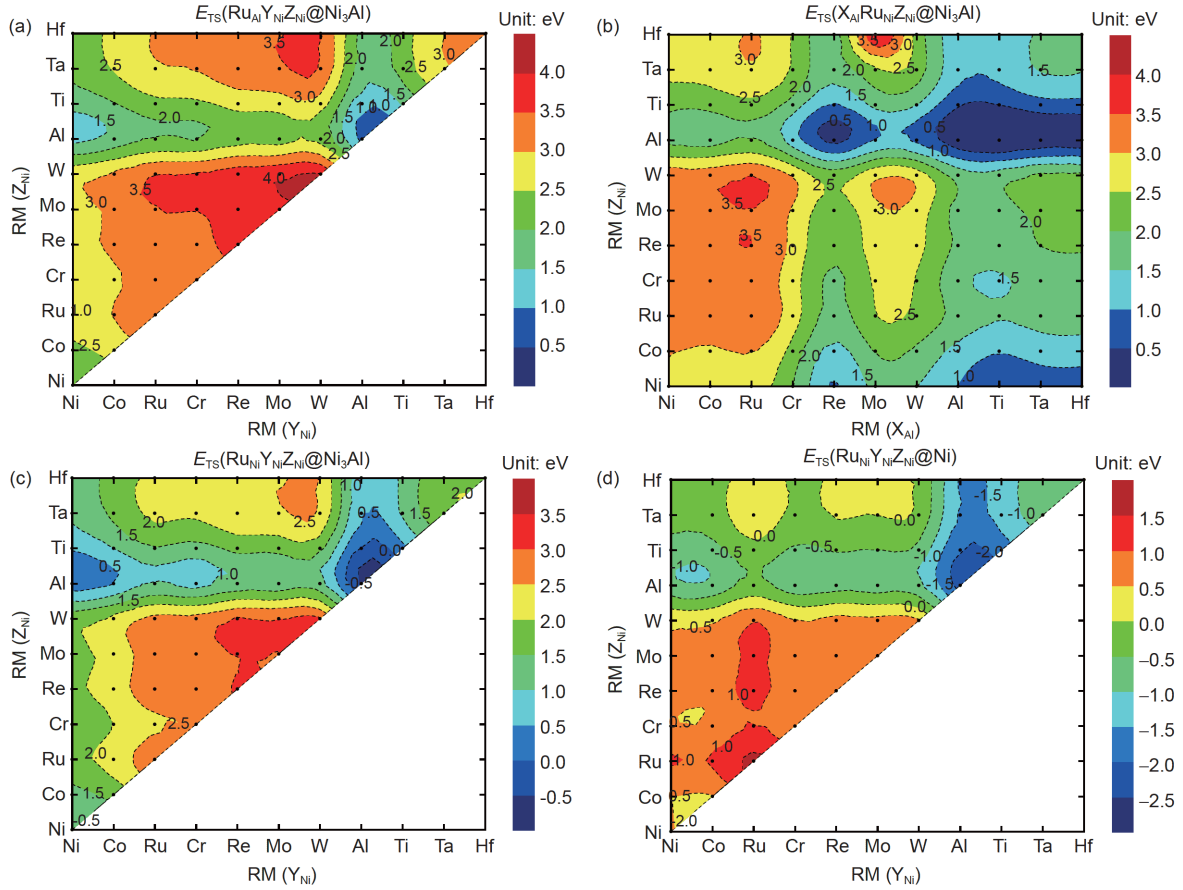

Figure 5 (Color online) Triple-site substitution energies of RuYZ or XRuZ substitutions for the four non-equivalent triple-site configurations of Ni and Ni_3Al. (a) $Ru_{Al}Y_{Ni}Z_{Ni}@Ni_3Al$, (b) $X_{Al}Ru_{Ni}Z_{Ni}@Ni_3Al$, (c) $Ru_{Ni}Y_{Ni}Z_{Ni}@Ni_3Al$, and (d) $Ru_{Ni}Y_{Ni}Z_{Ni}@Ni$ where X, Y, and Z are one of the 11 alloying elements. X, Y, Z = Ni, Co, Ru, Cr, Re, Mo, W, Al, Ti, Ta, and Hf, sorted in the increasing order of metal radii.

figurations containing Ru, $Ru_{Ni}Y_{Ni}Z_{Ni}$@Ni are generally more stable than the other three configurations, indicating that Ru preferred to occupy Ni phase rather than Ni_3Al phase in the triple-site doping. $Ru_{Ni}Y_{Ni}Z_{Ni}$@Ni had negative E_{TS} when Y or/and Z= Al, Ti, Ta, and Hf with large metal radii. Among the four triple-site substitution configurations, $Ru_{Ni}Al_{Ni}Al_{Ni}$@Ni had the largest E_{TS}= −2.230 eV, followed by $Ru_{Ni}Al_{Ni}Al_{Ni}$@Ni_3Al (−0.604 eV), $Ti_{Al}Ru_{Ni}Al_{Ni}$@Ni_3Al (−0.125 eV), and $Ru_{Al}Al_{Ni}Al_{Ni}$@Ni_3Al (0.835 eV). We found again that the antisite defect Al_{Ni} stabilized Ru substitution in both Ni and Ni_3Al in the triple-site doping configurations, consistent with the results of the dual-site doping. Ru preferred to occupy Ni sites rather than Al sites in Ni_3Al, consistent with the results of the dual-site doping of Ru, but opposite to the site preference of Re occupancy.

3.2 Preference of phase and site occupancy with 11 alloying elements

3.2.1 Preference of phase occupancy in single-site doping

The single-site doping in the Ni and Ni_3Al phase has three non-equivalent occupancy sites, namely, $X_{Al}Ni_{Ni}Ni_{Ni}$@Ni_3Al, $Al_{Al}X_{Ni}Ni_{Ni}$@Ni_3Al, and $X_{Ni}Ni_{Ni}Ni_{Ni}$@Ni where X= Ni, Co, Ru, Cr, Re, Mo, W, Al, Ti, Ta, and Hf. Figure 6 shows the single-site substitution energy (E_{SS}) of these three doping configurations. By comparing E_{ss} in Ni and Ni_3Al, we found that all the studied alloying elements preferred to occupy Ni phase except that Re preferred to occupy the Al site of Ni_3Al in the case of single-site doping.

3.2.2 Preference of site occupancy in single-site doping of Ni_3Al

Ni_3Al lattice is composed of Ni and Al sublattices. By comparing the single-site substitution energies of Al and Ni sites, $E_{SS}(X_{Al}Ni_{Ni}Ni_{Ni}$@$Ni_3Al)$ vs. $E_{SS}(Al_{Al}X_{Ni}Ni_{Ni}$@$Ni_3Al)$, we can evaluate the preference of single-site doping in Ni_3Al. The results in Figure 6 show that Ni, Co, Ru, Cr, Al, and Ti alloying elements preferred to occupy Ni sites while Re, Mo, W, Ta, and Hf preferred to occupy Al sites in the single-site doping of Ni_3Al. These results are consistent with the most of available literature reports of the site preference of single-site doping in Ni_3Al. Lu et al. [4] found that Ti, Hf, Ta, Mo, W, and Re prefer to occupy the Al sites of Ni_3Al. Wu et al. [6] found that Mo, Re, Ta, W, Ti, and Nb prefer to occupy the Al sites of Ni_3Al. Zhou et al. [29] and Yu et al. [30] found that Re prefers to occupy the Al sites of Ni_3Al; Liu et al. [31] found that Ta prefers to occupy the Al sites of Ni_3Al. The transition metal elements with large metal radii prefer to occupy the Al sites of Ni_3Al.

We calculated the normalized transfer energies $\tilde{E}^{X}_{Al\to Ni}$ of 11 doping elements: $\tilde{E}^{Ni}_{Al\to Ni}$= 0, $\tilde{E}^{Co}_{Al\to Ni}$= 0.03, $\tilde{E}^{Ru}_{Al\to Ni}$= 0.30, $\tilde{E}^{Cr}_{Al\to Ni}$= 0.32, $\tilde{E}^{Re}_{Al\to Ni}$= 2.06, $\tilde{E}^{Mo}_{Al\to Ni}$= 1.80, $\tilde{E}^{W}_{Al\to Ni}$= 2.15, $\tilde{E}^{Al}_{Al\to Ni}$= 1, $\tilde{E}^{Ti}_{Al\to Ni}$= 0.41, $\tilde{E}^{Ta}_{Al\to Ni}$= 2.20, and $\tilde{E}^{Hf}_{Al\to Ni}$= 2.20. Among the 11 studied doping elements, Ni, Co, Ru, Cr, Al, and Ti preferred to occupy the Ni sites of Ni_3Al, while Re, Mo, W, Ta, and Hf preferred to occupy the Al sites of Ni_3Al. The tendency of doping elements occupying the Al sites of Ni_3Al decreases with the increasing number of d electrons.

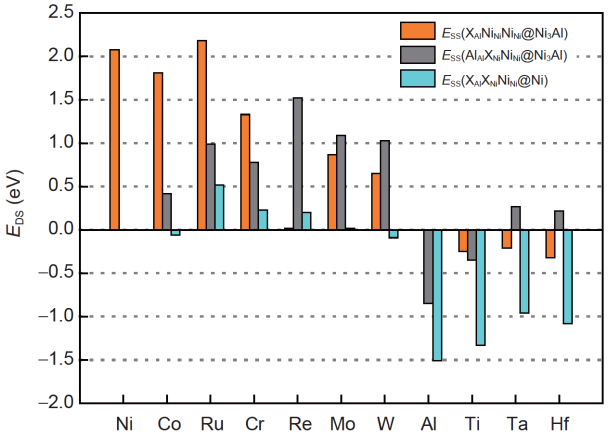

Figure 6 (Color online) Single-site substitution energies of the three non-equivalent occupancy sites in Ni and Ni_3Al: $X_{Al}Ni_{Ni}Ni_{Ni}$@Ni_3Al, $Al_{Al}X_{Ni}Ni_{Ni}$@Ni_3Al, and $X_{Ni}Ni_{Ni}Ni_{Ni}$@Ni where X= Ni, Co, Ru, Cr, Re, Mo, W, Al, Ti, Ta, and Hf.

3.2.3 Preference of site occupancy in dual-site doping

Considering 11 doping elements in Ni and Ni_3Al, there are four non-equivalent dual-site substitution configurations: $X_{Al}Y_{Ni}Ni_{Ni}$@Ni_3Al, $Al_{Al}X_{Ni}Y_{Ni}$@Ni_3Al, $X_{Ni}Y_{Ni}Ni_{Ni}$@Ni_3Al, and $X_{Ni}Y_{Ni}Ni_{Ni}$@Ni where X= Ni, Co, Ru, Cr, Re, Mo, W, Al, Ti, Ta, and Hf. All dual-site doping configurations preferred to occupy Ni phase rather than Ni_3Al phase.

Comparing the dual-site substitution energies E_{DS} in the two Ni_3Al configurations: $E_{DS}(X_{Al}Y_{Ni}Ni_{Ni}$@$Ni_3Al)$ and $E_{DS}(Al_{Al}X_{Ni}Y_{Ni}$@$Ni_3Al)$. The preference of site occupancy can be classified into the three cases as follows:

(1) When X= Ni, Co, Ru, Cr, and Al, XY dual-site doping preferred to occupy the NiNi sites rather than the AlNi sites;

(2) When X= Re, Mo, W, Ta, and Hf, XY dual-site doping preferred to occupy the AlNi sites rather than the NiNi sites;

(3) When X= Ti, if Y= Ni, Co, Ru, XY dual-site doping preferred to occupy the NiNi sites rather than the AlNi sites; if Y= Cr, Re, Mo, W, Al, Ti, Ta, and Hf with large metal radii, XY dual-site doping preferred to occupy the AlNi sites rather than the NiNi sites.

3.3 Preference of phase and site occupancy in triple-site doping

3.3.1 Preference of phase occupancy in triple-site doping

Considering the doping elements X, Y, Z= Ni, Co, Ru, Cr, Re, Mo, W, Al, Ti, Ta, and Hf, the comparison between E_{TS}

($X_{Ni}Y_{Ni}Z_{Ni}$@Ni_3Al) and E_{TS}($X_{Ni}Y_{Ni}Z_{Ni}$@Ni) shows the phase preference of the triple-site doping. The calculations of all the 220 triple-site substitution configurations showed all the studied alloying elements preferred to occupy Ni phase rather than Ni_3Al phase.

3.3.2 Preference of site occupancy in triple-site doping

By comparing E_{TS}($X_{Al}Y_{Ni}Z_{Ni}$@Ni_3Al) with E_{TS}($X_{Ni}Y_{Ni}Z_{Ni}$@Ni_3Al), the site preference of the triple-site doping in Ni_3Al can be examined. The preference of site occupancy in Ni_3Al is classified into the following three cases:

(1) When X= Ni, Co, Ru, Cr, Al, the XYZ triple-site doping preferred to occupy the NiNiNi sites rather than the AlNiNi sites;

(2) When X= Re, W, Ta, Hf, the XYZ triple-site doping in Ni_3Al preferred to occupy the AlNiNi sites rather than the NiNiNi sites;

(3) When X= Mo, Ti, if Y= Ni, Co, Ru, the XYZ triple-site doping in Ni_3Al preferred to occupy the NiNiNi sites rather than the AlNiNi sites; if Y= Cr, Re, Mo, W, Al, Ti, Ta, Hf, the XYZ triple-site doping in Ni_3Al preferred to occupy the AlNiNi sites rather than the NiNiNi sites.

Similar to Re and Ru the substitution energies of the other nine studied elements (Ni, Co, Cr, Mo, W, Al, Ti, Ta, and Hf) are shown in Figures S1–S9 for the dual-site doping and Figures S10–S18 for the triple-site doping. We found that the substitutions of Al, Ti, Ta, and Hf for the Ni site of Ni are energetically favorable and stabilized the substitution of any studied alloying elements for the other one or two sites in both dual-site and triple-site doping of Ni. The stabilization effects decreased in the order of Al_{Ni}> Ti_{Ni}> Ta_{Ni}~Hf_{Ni}, consistent with the decreasing order of the single-site doping energies: E_{SS}($Al_{Ni}Ni_{Ni}Ni_{Ni}$@Ni)=−1.511 eV, E_{SS}($Ti_{Ni}Ni_{Ni}Ni_{Ni}$@Ni)= −1.314 eV, E_{SS}($Ta_{Ni}Ni_{Ni}Ni_{Ni}$@Ni)= −0.941 eV, E_{SS}($Hf_{Ni}Ni_{Ni}Ni_{Ni}$@Ni)= −1.041 eV. The antisite Al_{Ni} is the most effective defect for stabilization probably due to the strong p-d orbital hybridization between Al and Ni.

4 Conclusions

To understand the preference of phase and site occupancy of alloying elements in Ni-based single crystal superalloys, we studied systematically the energy changes due to the substitution of 11 alloying elements in Ni and Ni_3Al, respectively, using density functional theory calculations. We considered the multiple doping at single-site (SS), dual-site (DS), and triple-site (TS) in Ni_3Al and Ni models, respectively. We calculated the substitution energies of 1298 substitution configurations in total including 726 AlNiNi site doping configurations ($X_{Al}Y_{Ni}Z_{Ni}$@Ni_3Al), 286 NiNiNi site doping configurations ($X_{Ni}Y_{Ni}Z_{Ni}$@Ni_3Al), and 286 NiNiNi site doping configurations ($X_{Ni}Y_{Ni}Z_{Ni}$@Ni) where X, Y, and Z= Ni, Co, Ru, Cr, Re, Mo, W, Al, Ti, Ta, and Hf. The main results are summarized as follows.

(1) In the single-site doping, all the studied alloying elements preferred to occupy Ni phase rather than Ni_3Al phase except that Re preferred to occupy the Al site of Ni_3Al. In the doping of Ni_3Al phase, Ni, Co, Ru, Cr, Al, and Ti elements preferred to occupy Ni sites while Re, Mo, W, Ta, and Hf elements preferred to occupy Al sites. When the metal radius of the doping element is larger than that of Al, the doping element preferred to occupy the Al site of Ni_3Al. The antisite defect Al_{Ni} is energetically favorable but the antisite defect Ni_{Al} is not stable in Ni_3Al.

(2) In the dual-site doping of Ni and Ni_3Al, all 55 configurations preferred to occupy Ni phase rather than Ni_3Al phase. The dual-site doping of Ni_3Al are classified into the following cases:

(i) When X= Ni, Co, Ru, Cr, and Al, XY dual-site doping preferred to occupy the NiNi sites rather than the AlNi sites independent of the type of Y elements;

(ii) When X= Re, Mo, W, Ta, and Hf, XY dual-site doping preferred to occupy the AlNi sites rather than the NiNi sites independent of the type of Y elements;

(iii) When X= Ti, if Y= Ni, Co, and Ru, XY dual-site doping preferred to occupy the NiNi sites; if Y= Cr, Re, Mo, W, Al, Ti, Ta, and Hf, XY dual-site doping preferred to occupy the AlNi sites.

(3) In the triple-site doping of Ni and Ni_3Al, all 220 configurations preferred to occupy Ni phase rather than Ni_3Al phase. The triple-site doping of Ni_3Al are classified into the following cases:

(i) When X= Ni, Co, Ru, Cr, and Al, the XYZ triple-site doping preferred to occupy the NiNiNi sites rather than the AlNiNi sites independent of the types of Y and Z elements;

(ii) When X= Re, W, Ta, and Hf, the XYZ triple-site doping preferred to occupy the AlNiNi sites rather than the NiNiNi sites independent of the types of Y and Z elements;

(iii) When X = Mo, Ti, if Y= Ni, Co, and Ru, the XYZ triple-site doping preferred to occupy the NiNiNi sites rather than the AlNiNi sites independent of the type of Z elements; if Y= Cr, Re, Mo, W, Al, Ti, Ta, and Hf, the XYZ triple-site doping preferred to occupy the AlNiNi sites rather than the NiNiNi sites independent of the type of Z elements.

We found the favorable substitutions of Al, Ti, Ta, and Hf for the Ni sites of Ni and Ni_3Al that stabilized the other studied alloying elements doping at the other one or two nearest neighbor sites of Ni. The strength of stabilization decreased in the order of Al_{Ni}> Ti_{Ni}> Ta_{Ni}~Hf_{Ni}. Among these alloying elements, the formation of Al_{Ni} antisite defect is most energetically favorable and stabilized the other element substitutions including Re and Ru in the dual-site and triple-site doping of both Ni and Ni_3Al. The most stable substitutions normally contained the primary substitutions of Al, Ti, Ta, and Hf for the Ni sites of Ni regardless of the other

alloying elements and doping sites. Such multiple substitutions should be considered as a whole defect complex in elaborating the mechanism of solution strengthening of the alloying elements. The defect complex containing multiple substitutions is critical to hindering the dislocation movement and enhance the dragging effects that increase the creep strength of superalloy. This work examined the multiple alloying effects on the substitution energies and the preference of phase and site occupancy up to the triple nearest neighbor substitution sites, helping to understand the strengthening mechanism of multiple alloying elements and the rational composition design for Ni-based single crystal superalloys.

This work was supported by the Independent Research and Development Project of State Key Laboratory of Advanced Special Steel, the Shanghai Key Laboratory of Advanced Ferrometallurgy, Shanghai University (Grant No. SKLASS 2019-Z024), the Science and Technology Commission of Shanghai Municipality (Grant No. 19DZ2270200), and the National Key Research and Development Program of China (Grant Nos. 2017YFB0701502 and 2017YFB0702901). Computations were carried out using the HPC facilities at Shanghai University, Shanghai Supercomputer Center, and Beijing Super Cloud Computing Center, China.

Supporting Information

The supporting information is available online at tech.scichina.com and link.springer.com. The supporting materials are published as submitted, without typesetting or editing. The responsibility for scientific accuracy and content remains entirely with the authors.

1 Caron P, Khan T. Evolution of Ni-based superalloys for single crystal gas turbine blade applications. Aerospace Sci Tech, 1999, 3: 513–523
2 Koizumi Y, Zhang J X, Kobayashi T, et al. Development of next generation Ni-base single crystal superalloys containing ruthenium. J Jpn Inst Met, 2003, 67: 468–471
3 Shibuya S, Kaneno Y, Tsuda H, et al. Microstructural evolution of dual multi-phase intermetallic alloys composed of geometrically close packed Ni_3X (X: Al and V) type structures. Intermetallics, 2007, 15: 338–348
4 Lu B K, Wang C Y, Du Z H. Site preferences of alloying transition metal elements in Ni-based superalloy: A first-principles study. Chin Phys B, 2018, 27: 532–540
5 Hashizume R, Yoshinari A, Kiyono T, et al. Development of novel Ni-based single crystal superalloys for power-generation gas turbines. Mater at High Temp, 2007, 24: 163–172
6 Wu Q, Li S. Alloying element additions to Ni_3Al: Site preferences and effects on elastic properties from first-principles calculations. Comput Mater Sci, 2012, 53: 436–443
7 Wang S Y, Wang C Y, Sun J H, et al. Energetics and electronic structure of Re and Ta in the γ′ phase of Ni-based superalloys. Phys Rev B, 2001, 65: 035101
8 Huang M, Zhu J. An overview of rhenium effect in single-crystal superalloys. Rare Met, 2016, 35: 127–139
9 Jiang C. Site preference of transition-metal elements in B2 NiAl: A comprehensive study. Acta Mater, 2007, 55: 4799–4806
10 Zhao W, Sun Z, Gong S. Synergistic effect of co-alloying elements on site preferences and elastic properties of Ni_3Al: A first-principles study. Intermetallics, 2015, 65: 75–80
11 Rawlings R D, Staton-Bevan A E. The alloying behaviour and mechanical properties of polycrystalline Ni_3Al (γ′ phase) with ternary additions. J Mater Sci, 1975, 10: 505–514
12 Chiba A, Hanada S, Watanabe S. Effect of γ and γ′ former doping on ductility of Ni_3Al. Scripta Metall Mater, 1991, 25: 303–307
13 Chiba A, Hanada S, Watanabe S. Ductilization of Ni_3 by microalloying with Ag. Scripta Metall Mater, 1992, 26: 1031–1036
14 Lu Y, Chen W, Eadie R. Evaluation of high temperature corrosion resistance of a Ni_3Al (Mo) alloy. Intermetallics, 2004, 12: 1299–1304
15 Sato A, Harada H, Yeh A C, et al. A 5th generation SC superalloy with balanced high temperature properties and processability. In: Proceedings of the 11th International Symposium on Superalloys. Pennsylvania, 2008. 131–138
16 Gleeson B, Wang W, Hayashi S, et al. Effects of platinum on the interdiffusion and oxidation behavior of Ni-Al-based alloys. Mater Sci Forum, 2004, 461-464: 213–222
17 Ge B H, Luo Y S, Li J R, et al. Distribution of rhenium in a single crystal nickel-based superalloy. Scripta Mater, 2010, 63: 969–972
18 Huang M, Cheng Z, Xiong J, et al. Coupling between Re segregation and γ/γ′ interfacial dislocations during high-temperature, low-stress creep of a nickel-based single-crystal superalloy. Acta Mater, 2014, 76: 294–305
19 Perdew J P, Burke K, Ernzerhof M. Generalized gradient approximation made simple. Phys Rev Lett, 1996, 77: 3865–3868
20 Huang Y, Mao Z, Noebe R D, et al. The effects of refractory elements on Ni-excesses and Ni-depletions at γ(f.c.c.)/γ′(L12) interfaces in model Ni-based superalloys: Atom-probe tomographic experiments and first-principles calculations. Acta Mater, 2016, 121: 288–298
21 Mottura A, Warnken N, Miller M K, et al. Atom probe tomography analysis of the distribution of rhenium in nickel alloys. Acta Mater, 2010, 58: 931–942
22 Liu S, Wen M, Li Z, et al. Partitioning and diffusion of transition metal solutes in ternary model Ni-based single crystal superalloys. Mater Des, 2017, 130: 157–165
23 Tan X P, Mangelinck D, Perrin-Pellegrino C, et al. Atom probe tomography of secondary γ′ precipitation in a single crystal Ni-based superalloy after isothermal aging at 1100°C. J Alloys Compd, 2014, 611: 389–394
24 Kresse G, Furthmüller J. Efficient iterative schemes for *ab initio* total-energy calculations using a plane-wave basis set. Phys Rev B, 1996, 54: 11169–11186
25 Blöchl P E. Projector augmented-wave method. Phys Rev B, 1994, 50: 17953–17979
26 Kresse G, Joubert D. From ultrasoft pseudopotentials to the projector augmented-wave method. Phys Rev B, 1999, 59: 1758–1775
27 Monkhorst H J, Pack J D. Special points for Brillouin-zone integrations. Phys Rev B, 1976, 13: 5188–5192
28 Ruban A V, Skriver H L. Calculated site substitution in ternary γ'-Ni_3Al: Temperature and composition effects. Phys Rev B, 1997, 55: 856–874
29 Zhou Y, Mao Z, Booth-Morrison C, et al. The partitioning and site preference of rhenium or ruthenium in model nickel-based superalloys: An atom-probe tomographic and first-principles study. Appl Phys Lett, 2008, 93: 171905
30 Yu X X, Wang C Y, Zhang X N, et al. Synergistic effect of rhenium and ruthenium in nickel-based single-crystal superalloys. J Alloys Compd, 2014, 582: 299–304
31 Liu S H, Liu C P, Liu W Q, et al. Investigation of the elemental partitioning behaviour and site preference in ternary model nickel-based superalloys by atom probe tomography and first-principles calculations. Philos Mag, 2016, 96: 2204–2218